JOURNAL OF GUIDANCE, CONTROL, AND DYNAMICS
Vol. 24, No. 5, September–October 2001

Practical Dual-Control Guidance Using Adaptive Intermittent Maneuver Strategy

Ho-Il Lee* and Min-Jea Tahk†
Korea Advanced Institute of Science and Technology, Taejon 305-701, Republic of Korea
and
Byung-Chan Sun‡
Korea Aerospace Research Institute, Taejon 305-333, Republic of Korea

A new adaptive intermittent maneuver strategy is proposed, which has switching threshold levels dependent on the estimated time-to-go for dual-control guidance of passive homing missiles. Guidance performance in terms of control effort and target observability for the adaptive intermittent maneuver strategy are also analyzed, as well as proportional navigation guidance. With intermittent maneuvers the guidance command is occasionally disabled to intentionally increase guidance errors. When provided with suitable switching threshold levels, this intermittent maneuver strategy improves target observability and, consequently, intercept performance. Statistical simulations for an atmospheric engagement demonstrate the effectiveness of the proposed intermittent maneuver strategy.

Introduction

In homing missiles equipped with a line-of-sight (LOS) angle sensor, target position and velocity are not measured directly, but must be estimated from LOS angle measurements using a target tracking filter.[1–5] With passive seekers, however, target observability is not guaranteed, but it is dependent on the relative motion of the target, which is in turn affected by the guidance activities of the missile. Previous studies[6,7] attempted to analyze this observability problem inherent to proportional navigation (PN) and augmented PN with passive seekers. The guidance problem with angle-only measurement is a dual-control (or stochastic control) problem for which control (or guidance) and estimation are not separable.

Although a rigorous solution to this problem has not yet been found, some dual-control guidance schemes have been devised: a dual-control strategy using two maneuvers for guidance parameter estimation and miss distance reduction was suggested in Ref. 8, and a linear-quadratic dual control was proposed in Ref. 9. Birmiwal and Bar-Shalom proposed an adaptive dual-control guidance based on an approximate solution of the stochastic dynamic programming equation to intercept moving target in the presence of a decoy.[10] Trajectory modulation techniques have also been developed to improve target observability under the assumption that better target observability would result in smaller miss distances. Such techniques are maximum-information guidance proposed in Refs. 11 and 12 and intermittent maneuver (IM) strategy studied in Refs. 13 and 14. An augmented proportional guidance law with a feedback of the LOS angle was also proposed in Ref. 7 to improve target observability.

IM strategy is a trajectory modulation technique for dual control, which intentionally increases LOS rates to a certain level by intermittently switching off the guidance commands. Reference 13 investigated a periodic IM scheme and found it effective in improving target observability. Motivated by this study, an adaptive intermittent maneuver (AIM) scheme with two threshold values of LOS rate was proposed in Ref. 14, where the two threshold levels serve as switching conditions; the upper threshold value determines when to activate the guidance command, and the lower value determines when to disable the command. However, this has some drawbacks such that the fixed threshold levels can cause a large miss distance because of large maneuver near the intercept point. To overcome these drawbacks, Ref. 15 proposes varying threshold levels based on the observability analysis of Ref. 6.

In this study we briefly review the results of target analysis presented in Ref. 6 and propose a new set of threshold curves considering both the intercept and observability conditions obtained in the previous studies.[6,15] Next, the conditions under which the proposed AIM would be stable are analyzed. We also propose a systematic approach for selecting the appropriate threshold curves through the analysis of control effort and observability for the AIM. Finally, the stochastic simulation results are presented for the evaluation of the proposed AIM.

Target Observability Analysis

Consider an engagement geometry in a two-dimensional plane depicted as Fig. 1. Let $\boldsymbol{r}(t)$ and $\boldsymbol{v}(t)$ denote the relative position and velocity vector, respectively, and $\boldsymbol{a}_t(t)$ and $\boldsymbol{a}_m(t)$ denote the target acceleration and missile acceleration vector, respectively. We can then write

$$\boldsymbol{r}(t) = \boldsymbol{r}(t_i) + (t - t_i)\boldsymbol{v}(t_i) + \int_{t_i}^{t} (t - \tau)[\boldsymbol{a}_t(\tau) - \boldsymbol{a}_m(\tau)]\,\mathrm{d}\tau \quad (1)$$

$$\boldsymbol{v}(t) = \boldsymbol{v}(t_i) + \int_{t_i}^{t} [\boldsymbol{a}_t(t) - \boldsymbol{a}_m(t)]\,\mathrm{d}\tau \quad (2)$$

where t_i is the initial time. We assume that the missile range, velocity, and acceleration are perfectly known. The LOS angle is defined by

$$\sigma = \tan^{-1}(r_z/r_x) \quad (3)$$

where r_x and r_z are the components of $\boldsymbol{r}(t)$; $\boldsymbol{r}(t) = [r_x \;\; r_z]^T$. Equation (3) can be written in the form of a pseudomeasurement:

$$\cos\sigma(t) r_z(t) - \sin\sigma(t) r_x(t) = 0 \quad (4)$$

Substitution of Eqs. (1) and (2) into Eq. (4) gives

$$M(t)\boldsymbol{x} = y(t) \quad (5)$$

where $M(t)$ and $y(t)$ are determined from the LOS angle and missile acceleration, respectively, and $\boldsymbol{x}$, which consists of the initial conditions of the target model, is an $n \times 1$ constant vector to be observed. The size of $\boldsymbol{x}$ depends on the number of the state variables of target model.

Received 28 April 2000; revision received 12 October 2000; accepted for publication 10 November 2000.

*Graduate Student, Division of Aerospace Engineering.
†Professor, Division of Aerospace Engineering.
‡Senior Researcher, Guidance and Control Department.

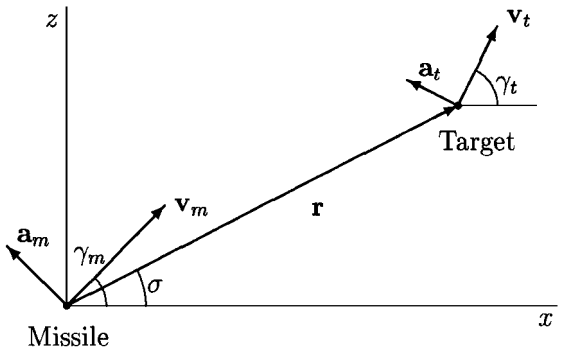

Fig. 1 Engagement geometry.

It is known that $\boldsymbol{x}$ is uniquely determined from the history of $\sigma(t)$ if and only if a matrix $A(t)$ defined as

$$A(t) = \begin{bmatrix} M(t) \\ \dot{M}(t) \\ \vdots \\ M^{(n-1)}(t) \end{bmatrix} \tag{6}$$

attains full rank at some $t > t_i$; that is,

$$\det[A(t)] \neq 0 \qquad \text{for} \qquad t > t_i \tag{7}$$

For convenience, we refer to $\mathcal{O} \equiv \det[A(t)]$ as the observability determinant. When the target velocity is constant, the target motion is described by a two-state equation of motion and the observability determinant is calculated as[16]

$$\mathcal{O}_{\text{cv}} = 2\dot{\sigma}\sigma^{(3)} - 3\ddot{\sigma}^2 + 4\dot{\sigma}^4 \tag{8}$$

where subscript cv stands for constant velocity (CV) target model. Analogously, when the target moves with constant acceleration, the equation of motion has three states and the observability determinant is[6]

$$\begin{aligned}\mathcal{O}_{\text{ca}} &= 18\ddot{\sigma}^2\sigma^{(5)} - 12\dot{\sigma}\sigma^{(3)}\sigma^{(5)} - 24\dot{\sigma}^4\sigma^{(5)} - 60\ddot{\sigma}\sigma^{(3)}\sigma^{(4)} \\ &\quad + 15\dot{\sigma}\sigma^{(4)^2} + 240\dot{\sigma}^3\ddot{\sigma}\sigma^{(4)} + 40\sigma^{(3)^3} - 720\dot{\sigma}^2\ddot{\sigma}^2\sigma^{(3)} \\ &\quad - 192\dot{\sigma}^6\sigma^{(3)} + 540\dot{\sigma}\ddot{\sigma}^4 + 288\dot{\sigma}^5\ddot{\sigma}^2 - 64\dot{\sigma}^9\end{aligned} \tag{9}$$

where ca stands for constant acceleration (CA) target model. The concrete derivations of Eqs. (8) and (9) are given in the references.

AIM Strategy with Varying Threshold Levels

Assume that the missile and the target are point-mass models with constant velocities. Then homing guidance equations in a relative polar coordinate system can be given as follows (Fig. 1):

$$\begin{aligned}\dot{r} &= v_t\cos(\gamma_t - \sigma) - v_m\cos(\gamma_m - \sigma) \\ r\dot{\sigma} &= v_t\sin(\gamma_t - \sigma) - v_m\sin(\gamma_m - \sigma) \\ \dot{\gamma}_m &= a_m/v_m, \qquad \dot{\gamma}_t = a_t/v_t\end{aligned} \tag{10}$$

For a nonmaneuvering target the kinematic relationship of the LOS angle in the polar coordinates is given by

$$\ddot{\sigma} = (-2\dot{r}\dot{\sigma} - a_{m\perp})/r \tag{11}$$

where $a_{m\perp}$ is the acceleration component of the missile normal to the LOS. With true proportional navigation (TPN) the commanded missile acceleration normal to the LOS is given by

$$a_{m\perp_c} = -N\dot{r}\dot{\sigma} \tag{12}$$

where N denotes the guidance gain. We consider a point-mass missile model for which the dynamics of the missile airframe and autopilot are neglected, that is, $a_{m\perp} = a_{m\perp_c}$. We also assume an intercept scenario for which the closing velocity is constant: $\ddot{r} = 0$. Substitution of Eq. (12) into Eq. (11) gives

$$\ddot{\sigma} = (N-2)(\dot{r}/r)\dot{\sigma} \tag{13}$$

Now substitute Eq. (13) and its higher-order derivatives into the expressions of the observability determinants Eqs. (8) and (9) to obtain

$$\mathcal{O}_{\text{cv}} = -N(N-2)\kappa^2\dot{\sigma}^2 + 4\dot{\sigma}^4 \tag{14}$$

$$\begin{aligned}\mathcal{O}_{\text{ca}} &= (N+1)N^2(N-2)^2(N-3)\kappa^6\dot{\sigma}^3 + 36(N^2-2N+2) \\ &\quad \times N(N-2)\kappa^4\dot{\sigma}^5 + 96N(N-2)\kappa^2\dot{\sigma}^7 - 64\dot{\sigma}^9\end{aligned} \tag{15}$$

where $\kappa = \dot{r}/r$. To investigate the significance of each term in the preceding expressions, we integrate Eq. (13) to obtain

$$\dot{\sigma}/\dot{\sigma}_0 = (r/r_0)^{N-2} \tag{16}$$

where subscript 0 denotes the values at the time of activating the guidance command. Now substitute Eq. (16) into Eqs. (14) and (15) to obtain the observability determinants expressed in terms of $\dot{\sigma}_0$, r_0, and r as

$$\mathcal{O}_{\text{cv}} = -N(N-2)\kappa_0^2\dot{\sigma}_0^2\rho^{2N-6} + 4\dot{\sigma}_0^4\rho^{4N-8} \tag{17}$$

$$\begin{aligned}\mathcal{O}_{\text{ca}} &= (N+1)N^2(N-2)^2(N-3)\kappa_0^6\dot{\sigma}_0^3\rho^{3N-12} \\ &\quad + 36(N^2-2N+2)N(N-2)\kappa_0^4\dot{\sigma}_0^5\rho^{5N-14} \\ &\quad + 96N(N-2)\kappa_0^2\dot{\sigma}_0^7\rho^{7N-16} - 64\dot{\sigma}_0^9\rho^{9N-18}\end{aligned} \tag{18}$$

where $\kappa_0 = \dot{r}/r_0$ and $\rho = r/r_0$. We observe that under PN guidance the observability determinants are expressed by the form $\mathcal{O} = \sum c_j\rho^{n_j}$, where the constants c_j and exponents n_j depend on the choice of guidance gain and target model. The ratio of the first term of $\mathcal{O}_{\text{cv}}$ to the second term is proportional to ρ^{-2N+2}. Because $\rho \to 0$ as $t \to t_f$, where t_f is defined as the terminal time for which $r(t_f) = 0$, we see that if $N > 1$ the first term becomes dominating $\mathcal{O}_{\text{cv}}$ as $t \to t_f$. Using similar arguments for $\mathcal{O}_{\text{ca}}$, we can easily identify its first term as the dominant one. Hence, it is reasonable to approximate the observability determinants as

$$\mathcal{O}_{\text{cv}} \approx -N(N-2)\kappa_0^2\dot{\sigma}_0^2\rho^{2N-6} \tag{19}$$

$$\mathcal{O}_{\text{ca}} \approx (N+1)N^2(N-2)^2(N-3)\kappa_0^6\dot{\sigma}_0^3\rho^{3N-12} \tag{20}$$

The guidance command is calculated using the state variables of Eq. (10), all of which are not measured. This brings the need to use a state estimator to obtain the guidance command using the estimated variables. To generate reliable guidance command, it is necessary to modulate the intercept trajectory to enhance the observability of the system given as Eq. (10). The AIM strategy proposes the time of turning on and off the guidance command by comparing the current value of an index variable, which affects the target observability with threshold levels. We select the LOS rate as the index variable based on the target observability in Eqs. (19) and (20). Let $\dot{\sigma}_U$ and $\dot{\sigma}_L$ denote positive upper and lower threshold levels, respectively. Then we can define an AIM switching function in the following:

Definition 1: Let $\{t_\ell\}$ be the sequence of times to update the guidance command. Then the AIM switching sequence $\{\mathcal{S}_\ell\}$ is defined as

$$\mathcal{S}_0 = \begin{cases} 1, & \text{if} \quad |\dot{\sigma}(t_\ell)| > \dot{\sigma}_L \\ 0, & \text{if} \quad |\dot{\sigma}(t_\ell)| \leq \dot{\sigma}_L \end{cases} \tag{21}$$

and for all $\ell \geq 1$

$$\mathcal{S}_\ell = \begin{cases} 1, & \text{if} \quad |\dot{\sigma}(t_\ell)| \geq \dot{\sigma}_U \\ \mathcal{S}_{\ell-1}, & \text{if} \quad \dot{\sigma}_L < |\dot{\sigma}(t_\ell)| < \dot{\sigma}_U \\ 0, & \text{if} \quad |\dot{\sigma}(t_\ell)| \leq \dot{\sigma}_L \end{cases} \tag{22}$$

Furthermore, the AIM switching function is defined as

$$\mathcal{S}(t) = \mathcal{S}_\ell, \qquad t_\ell \leq t < t_{\ell+1} \tag{23}$$

The key point in designing an AIM scheme is how to choose the upper and lower threshold levels. The lower threshold level

should prohibit target observability from decreasing too low. The upper threshold should be carefully selected by the considering the missile's maneuvering capability. If the upper threshold is too high, large guidance errors can be produced, and large missile maneuvers are required to recover these errors. The threshold curves should satisfy two conditions:

1) The $\dot{\sigma}_U$ goes to 0 as $t_{go} \to 0$.

2) The magnitude of the observability determinant on the lower threshold monotonically increases as $t_{go} \to 0$.

The first condition is necessary to make the commanded acceleration reduce to zero at the terminal time, which is important in minimizing miss distance. The second condition is imposed to increase target observability near the end of the engagement. Accurate target state estimation becomes more important as the missile approaches the target if the effects of the target's evasive maneuvers and measurement noise are to be suppressed. For the first condition we choose an upper threshold curve as

$$\dot{\sigma}_U = \mu_U r^k, \qquad k > 0 \tag{24}$$

where μ_U is chosen from the initial conditions of engagement. In the following, we explain how to choose k from the second condition. The upper threshold determines when to resume the guidance law. Once the guidance law is activated, the observability determinant on the upper threshold for each model is obtained by substituting Eq. (24) into Eqs. (19) and (20) with $\rho = 1$ as

$$\mathcal{O}_{cv} = -N(N-2)\,\dot{r}^2 \mu_U^2\, r^{2(k-1)} \tag{25}$$

$$\mathcal{O}_{ca} = (N+1)N^2(N-2)^2(N-3)\dot{r}^6 \mu_U^3\, r^{3(k-2)} \tag{26}$$

It can easily be shown that the second condition for the threshold curves is satisfied if k is chosen as

$$0 < k < 1, \qquad \text{for CV model}$$

$$0 < k < 2, \qquad \text{for CA model} \tag{27}$$

for each target model. The lower threshold can be chosen in the same fashion as

$$\dot{\sigma}_L = \mu_L r^k \tag{28}$$

where μ_L must be less than μ_U.

From the preceding definitions of the threshold levels, we can define the switching region of AIM.

Definition 2: Let the threshold levels be as Eqs. (24) and (28). Then $\mathcal{A} = \{0 < r \le r_0)\} \times \{\dot{\sigma}_L(r) \le |\dot{\sigma}(r)| \le \dot{\sigma}_U(r)\}$ is called switching region of AIM (Fig. 2).

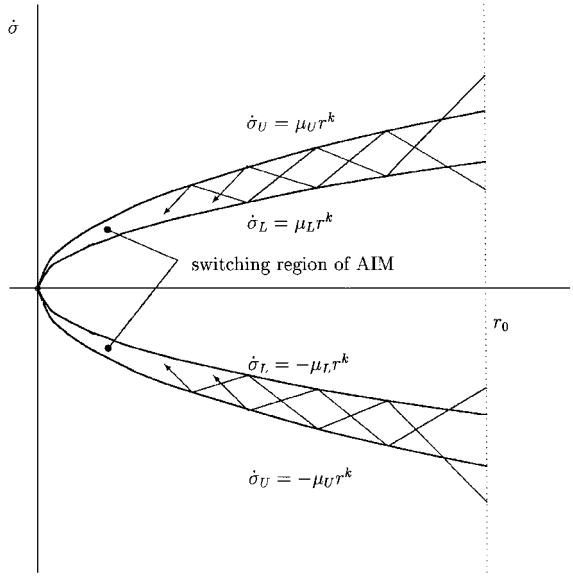

Fig. 2 Switching region of AIM.

Now, we prove that when the PN is applied as a guidance law, the trajectory $(r, \dot{\sigma})$ goes into the switching region of AIM and converges to the origin of the relative coordinate within that region. This is required to satisfy the target interception as well as to maintain a certain level of the target observability. If the velocity of the missile is greater than that of a target, it is possible to have $\dot{r} < 0$. This assumption is generally applied in the design of short-range homing guidance laws.

Lemma 1: Consider the system Eq. (10), and $0 < r \le r_0$. Suppose $a_t = 0$, and $\dot{r} < 0$. Let $a_{m\perp} = -\mathcal{S}(t)N\dot{r}\dot{\sigma}$ where $\mathcal{S}(t)$ is given by Eq. (23) and k satisfies Eq. (27). If $N > k+2$, then the intercept trajectory $(r, \dot{\sigma})$ reaches the switching region of AIM in finite time and remains inside thereafter.

Proof: Let $\dot{\sigma}_b = \mu_b r^k$, where $\mu_L < \mu_b < \mu_U$. Define a new variable z as $z = |\dot{\sigma}| - \dot{\sigma}_b$. Consider a positive function as $V(z) = z^2/2$. Then $\dot{V}(z)$ becomes

$$\dot{V}(z) = (z\dot{r}/r)\left\{[\mathcal{S}(t)N - 2]|\dot{\sigma}| - \mu_b k r^k\right\}, \qquad \text{for} \quad \dot{\sigma} \neq 0 \tag{29}$$

If $|\dot{\sigma}| \ge \dot{\sigma}_U$, then $\mathcal{S}(t) = 1$, and $z > 0$. Therefore, the inequality $N > k+2$ gives

$$\dot{V}(z) < (z\dot{r}k/r)\left(|\dot{\sigma}| - \mu_b r^k\right) = kz^2\dot{r}/r < 0 \tag{30}$$

If $0 < |\dot{\sigma}| \le \dot{\sigma}_L$, then $\mathcal{S}(t) = 0$, and $z < 0$

$$\dot{V}(z) = -(z\dot{r}/r)\left(2|\dot{\sigma}| + \mu_b k r^k\right) < 0 \tag{31}$$

If $\dot{\sigma} = 0$, then $z = -\dot{\sigma}_b$, and $\dot{V}(z) = kz^2\dot{r}/r < 0$. This implies that when the trajectory starts at $\dot{\sigma} = 0$ the trajectory converges to the origin to belong to the line of $\dot{\sigma} = 0$. This is a trivial case because its neighbors do not converge to the line.

Outside of the switching region of AIM except $\dot{\sigma} = 0$, we have $\dot{V}(z) < 0$. This implies that whenever $z(0) = \dot{\sigma}(0) - \dot{\sigma}_b(0) \notin \mathcal{A}$, $|z|$ will be strictly decreasing until it reaches region $\mathcal{A}$ in finite time. Inside of the switching region of AIM, $z = 0$ is not an invariant set so that $V(z)$ does not stay at zero. But because $V(z)$ is continuous and $\dot{V}(z)$ is negative out of the switching region of AIM, z is bounded, which implies that for all $[r(0), \dot{\sigma}(0)] \in \mathcal{A}$, the trajectory $(r, \dot{\sigma})$ is bounded for all $t \ge 0$.

Note that $\dot{\sigma}_U \to \dot{\sigma}_L \to 0$ as $t \to t_f$, then $\dot{\sigma} \to 0$. This implies that the AIM strategy causes the trajectory converge to the origin (Fig. 2). □

Lemma 1 states the conditions under which the states reach the region of AIM. If the states reach the region of AIM, the trajectories are enhanced observability by switching action. Otherwise, the trajectories simply intercept the origin without observability enhancement.

In practical applications the AIM strategy does not switch precisely on the thresholds caused by the presence of the actuator time delay and aerodynamics of missiles. Furthermore, as $t \to t_f$, the switching frequency of AIM diverges as the missile approaches to the target, and the guidance command can become unstable. In the following, the switching frequency of AIM is analyzed, and the condition under which the AIM strategy is stable is discussed.

Consider an AIM guidance strategy as displayed in Fig. 3. Here, the guidance kinematics begin at the upper threshold. Assume that a missile is guided under the PN with AIM, with guidance kinematics beginning at the upper threshold and that the closing velocity, V_c is constant. Only the CV target model is considered here. Then the relationship between the relative range and LOS rate is given by Eq. (16). In Fig. 3 define the range ratio of transition from on to off for cycle j, α, as

$$\alpha \triangleq \frac{r_{j,\text{off}}}{r_{j,\text{on}}} = \left(\frac{\mu_L}{\mu_U}\right)^{1/(N-2-k)} \tag{32}$$

Similarly, the range ratio of transition from off to on is given as $r_{j,\text{on}}/r_{j,\text{off}} = (\mu_L/\mu_U)^{1/(2+k)}$. Thus, the range ratio during an on–off cycle β is

$$\beta \triangleq \frac{r_{j+1,\text{on}}}{r_{j,\text{on}}} = \left(\frac{\mu_L}{\mu_U}\right)^{N/(N-2-k)(2+k)} \tag{33}$$

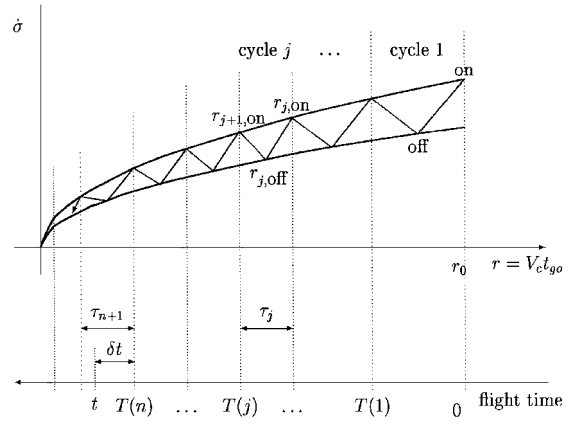

Fig. 3 Schematic diagram of AIM strategy.

Accordingly, the relative range after j AIM cycles can be expressed as

$$r_{j,\text{on}} = \beta^j r_0, \qquad \text{for} \qquad i = 1, 2, \ldots \tag{34}$$

In this case the switching function varies with respect to time depicted as lower part of Fig. 3. Current time t can be expressed as

$$t = T(n) + \delta t, \qquad \delta t > 0 \tag{35}$$

where

$$T(n) = \sum_{j=0}^{n} \tau_j$$

and τ_j is the period of the jth AIM cycle. $T(n)$ is the time taken for n AIM cycles, and δt is the time after $t = T(n)$. From $r_0 = V_c T(n) + \beta^n r_0$, we can obtain $T(n)$ as

$$T(n) = (1 - \beta^n) t_f \tag{36}$$

where t_f is the total flight time. Then,

$$\tau_{n+1} = T(n+1) - T(n) = \beta^n (1 - \beta) t_f \tag{37}$$

On the other hand, Eqs. (35) and (36) give

$$\beta^n = (t_f - t + \delta t)/t_f = (t_{\text{go}} + \delta t)/t_f \tag{38}$$

Substitution of Eq. (38) into Eq. (37) gives the switching frequency for current AIM cycle:

$$2\pi/\tau_{n+1} = 2\pi/[(t_{\text{go}} + \delta t)(1 - \beta)] \tag{39}$$

The switching frequency of AIM must be less than the system or the actuator bandwidth to maintain the stability. This is expressed as the following inequality:

$$t_{\text{go}} > 2\pi/\omega_b (1 - \beta) - \delta t \tag{40}$$

The preceding condition implies that if $t_{\text{go}} > 2\pi/[\omega_b(1 - \beta)]$ the AIM strategy works successfully; otherwise, the guidance performance and stability are not guaranteed.

Control Effort and Observability Enhancement Characteristic of AIM

Although AIM strategy enhances target observability, it can consume more control effort than do conventional guidance laws such as the PN. To prevent excessive control effort as well as to enhance observability, the parameters of AIM should be carefully selected. Using Eqs. (32–34), we now analyze the control effort and observability enhancement of AIM. Define the control effort as

$$E_p = \int_{t_i}^{t_f} |a_{m\perp}|^p \, \mathrm{d}t \tag{41}$$

where p is a constant and $a_{m\perp} = -\mathcal{S}(t) N \dot{r} \dot{\sigma}$. The control effort for jth cycle can be expressed as

$$E_{p,j} = \int_{t_{j,\text{on}}}^{t_{j,\text{off}}} N^p V_c^p \dot{\sigma}^p \, \mathrm{d}t \tag{42}$$

where V_c is the closing velocity $V_c = \dot{r}$. Provided $\ddot{r} = 0$, the total control effort for the AIM E_p^{AIM} can be given as

$$E_p^{\text{AIM}} = \sum_{j=0}^{\infty} E_{p,j} = \xi r_0^{pk+1} \frac{1 - \alpha^{p(N-2)+1}}{1 - \beta^{pk+1}} \tag{43}$$

where $\xi = \mu_U^p N^p V_c^{(p-1)}/[p(N-2)+1]$. Because μ_L is zero for the PN, the total control effort for the PN is

$$E_p^{\text{PN}} = \xi r_0^{pk+1} \tag{44}$$

Therefore, the ratio of the control effort is given by

$$\frac{E_p^{\text{AIM}}}{E_p^{\text{PN}}} = \frac{1 - \alpha^{p(N-2)+1}}{1 - \beta^{pk+1}} \tag{45}$$

To evaluate the observability enhancement, a certain observability measure is needed. Hull et al. proposed an observability performance index weighted by the relative range.[9] Similarly, we defined an observability performance index as the magnitude of observability determinant weighted by the time to go. Define observability measures weighted by t_{go} as

$$J_q = \int_{t_i}^{t_f} |\mathcal{O}_{\text{cv}}| \, t_{\text{go}}^q \, \mathrm{d}t \tag{46}$$

The weighting factor t_{go}^q is introduced to account for the fact that good target observability should be maintained for some time interval to yield a good target estimate. For the linearized geometry with the IM scheme, the observability determinant at the time of departure from the upper threshold is given by Eq. (25). Straightforward calculation for jth cycle gives

$$J_{q,j} = \eta r_j^{2k+q-1} (1 - \alpha^{2N-5+q}) \tag{47}$$

where $\eta = [N(N-2)/(2N-5+q)] \mu_U^2 V_c^{1-q}$. Total observability measure J_q^{AIM} is calculated by

$$J_q^{\text{AIM}} = \sum_{j=0}^{\infty} J_{q,j} = \eta r_0^{2k+q-1} \frac{1 - \alpha^{2N-5+q}}{1 - \beta^{2k+q-1}} \tag{48}$$

Because $\alpha = 0$ for the PN, J_q^{PN} is

$$J_q^{\text{PN}} = \eta r_0^{2k+q-1} \tag{49}$$

Hence, the ratio of the observability of the PN to AIM is given by

$$\frac{J_q^{\text{AIM}}}{J_q^{\text{PN}}} = \frac{1 - \alpha^{2N-5+q}}{1 - \beta^{2k+q-1}} \tag{50}$$

For improved observability J_q^{AIM} must be greater than J_q^{PN}; this condition gives

$$(\mu_L/\mu_U)^{(2N-5+q)/(N-2-k)} < (\mu_L/\mu_U)^{N(2k+q-1)/(N-2-k)(2+k)} \tag{51}$$

The condition is satisfied if

$$N - k - 2 > 0, \qquad q < 5 \tag{52}$$

Table 1 AIM performance ratio with respect to the guidance gains and the types of thresholds

k	$N=3$	$N=4$	$N=5$	(Type)
0^+	2.00	2.50	2.80	(Constant)
0.5	1.25	1.56	1.75	(Parabolic)
1^-	1.00	1.25	1.40	(Linear)

The first condition of Eq. (52) is equivalent to the condition to stay in the switching region of AIM. We can obtain asymptotic performance ratios as μ_L/μ_U goes to 1.

$$\frac{E_p^{\text{AIM}}}{E_p^{\text{PN}}} = \frac{[p(N-2)+1](2+k)}{N(pk+1)} \tag{53}$$

$$\frac{J_q^{\text{AIM}}}{J_q^{\text{PN}}} = \frac{(2N-5+q)(2+k)}{N(2k+q-1)} \tag{54}$$

For the specific case when $p=q=2$, we can define the AIM performance ratio:

$$\frac{E_2^{\text{AIM}}}{E_2^{\text{PN}}} = \frac{J_2^{\text{AIM}}}{J_2^{\text{PN}}} = \frac{(2N-3)(2+k)}{N(2k+1)} \tag{55}$$

The ratio of control energy is identical to that of observability enhancement in this case. Table 1 shows the AIM performance ratio for some selected threshold shapes such as constant, parabolic, and linear, and for some guidance gains.

Simulation Study

In this section the proposed AIM strategy is augmented to the PN and tested through statistical simulations. The missile is fired in the direction of the X axis with initial velocity of 550 m/s and is guided by TPN. The target is initially located at (2000, 1000 m) and moves at a constant speed of 200 m/s along the X axis. In addition to a constant velocity target, we also consider a maneuvering target to demonstrate the effectiveness of the AIM. Four different simulations are considered with the target model and the tracking filter of the missile: case 1: constant velocity target, model-CV filter; case 2: brief target maneuver near terminal time, model-CV filter; case 3: constant velocity target, model-CA filter; and case 4: brief target maneuver near terminal time, model-CA filter. Cases 2 and 4 are included to investigate the target observability enhancement characteristic of AIM strategy in the presence of unmodeled target motions. When the target flies with a constant velocity, the estimation errors become larger. At this time a small target maneuver can produce a large miss distance. A constant lateral target acceleration of -15 m/s^2 near the final time for about 1s is considered in these cases.

Target states are estimated using the modified-gain pseudomeasurement filter in Refs. 4 and 13. The filter state vectors of the model-CV and model-CA filters are $\hat{\boldsymbol{x}}_T = [r_x \;\; r_z \;\; v_x \;\; v_z]^T$ and $[r_x \;\; r_z \;\; v_x \;\; v_z \;\; a_{tx} \;\; a_{tz}]^T$, respectively. For the model-CV filter (cases 1 and 2) the initial target state estimate and covariance $\hat{P}(0)$ are set as $\hat{\boldsymbol{x}}_T(0) = [1000, 0, 100, 0]^T$ and $\text{diag}[\hat{P}(0)] = [1000^2, 1000^2, 1000^2, 1000^2]$, respectively. For the model-CA filter (cases 3 and 4) $\hat{\boldsymbol{x}}_T(0) = [1000, \; 0, \; 100, \; 0, \; 0, \; 0]^T$ and $\text{diag}[\hat{P}(0)] = [10{,}000^2, 10{,}000^2, 1000^2, 1000^2, 100^2, 100^2]$, respectively. LOS angle measurements are sampled at 20 Hz and corrupted by a white Gaussian noise sequence with zero mean and variance 9 (m rad)^2. The total time delay of the guidance loop is assumed as 0.1 s. To show well the performance of the AIM, a somewhat large noise were used for simulations. Threshold levels are chosen as Eqs. (24) and (28), where k are used 0.5 (model CV) and 1.0 (model CA). μ_U and μ_L are calculated from the initial condition of the engagement: $\dot{\sigma}_U(0) = 5.5$, and $\dot{\sigma}_L(0) = 4.0$ deg/s at $r = r(0)$.

The threshold levels are implemented using estimated range $\hat{r}$ and estimated time to go $\hat{t}_{\text{go}}$. The performance of the PN is tested with and without the AIM strategy for all cases. For each case 100 stochastic simulations are conducted with three different guidance gains as $N = 3$, 4, and 5.

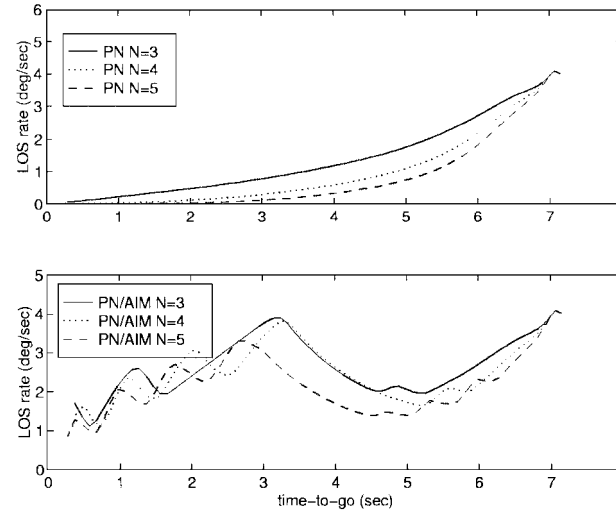

Fig. 4 LOS rates vs time to go (case 1).

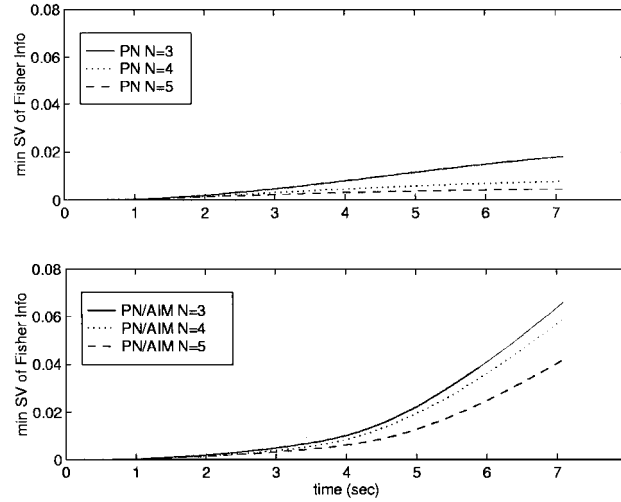

Fig. 5 Minimum singular values of Fisher information matrices (case 1).

Figures 4–6 are the averaged LOS rate, minimum singular value of the Fisher information matrix, which generally indicates the target observability,[11] and range estimate for case 1, respectively. In these figures the upper graph is for PN without AIM, the lower graph is for the AIM strategy with time-varying thresholds, denoted as PN/AIM. The switching property of the AIM strategy is evident in Fig. 4, where the LOS rate is seen to cross over the threshold levels caused by the time delay of the guidance loop. Figure 5 shows that the nonsingularity of the Fisher information matrix for the AIM scheme increases more rapidly than for PN. As shown in Fig. 6, the target tracking performance is slightly improved by the AIM scheme; especially, the range estimation error converges to zero near the terminal time.

Because the target motion precisely agrees with the target model for case 1, the target need not be observable at all times if there is no measurement error. In the presence of measurement noise, however, target observability near the terminal time is important. In the case of PN, the target becomes almost unobservable as t_{go} goes to 0. Hence, estimation errors caused by measurement noise are not readily reduced, resulting in poor miss-distance performance as shown in Fig. 7. The percentage of Y axis in this figure is calculated by

$$\text{percentage} = \text{Prob. of } \{\text{miss distance} \le \text{value of X axis}\} \times 100$$

This figure also shows that the AIM strategy produces a significant improvement in the intercept performance of PN via observability enhancement.

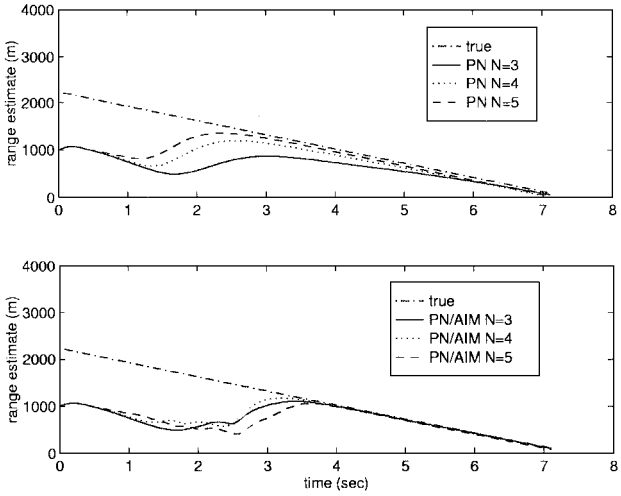

Fig. 6 Range estimation performance (case 1).

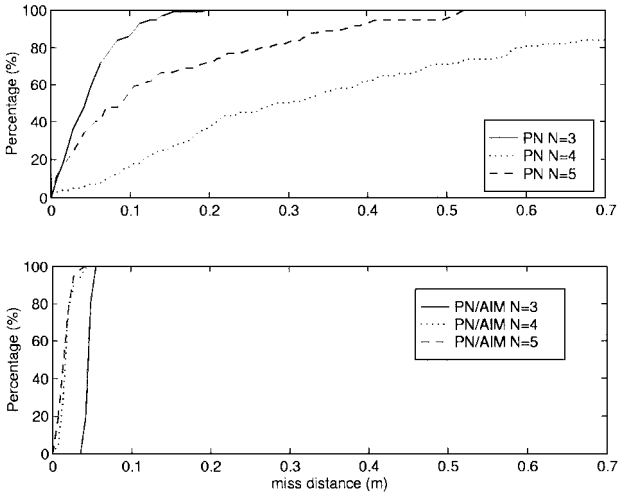

Fig. 7 Miss-distance statistics (case 1).

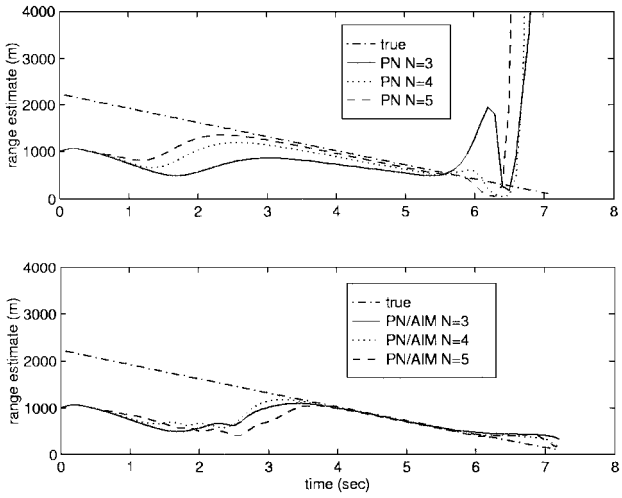

Fig. 8 Range estimation performance (case 2).

The effectiveness of the proposed AIM strategy is significant for case 2, which has a target maneuver near the terminal time. However, the estimation and miss-distance performance is quite different; the range estimation error diverges for PN. Consequently, the miss-distance characteristics of case 1 are completely destroyed by the target maneuver, as clearly seen in Figs. 8 and 9. On the other hand, if PN/AIM is used, the presence of target maneuvers produces neither unbounded estimation errors nor unacceptable increases in miss distance.

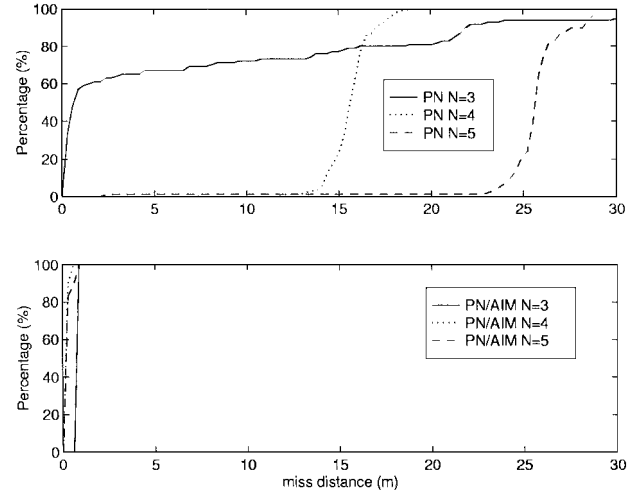

Fig. 9 Miss-distance statistics (case 2).

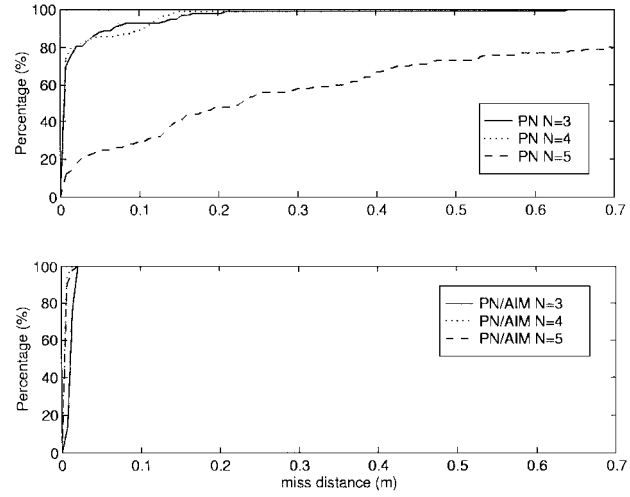

Fig. 10 Miss-distance statistics (case 3).

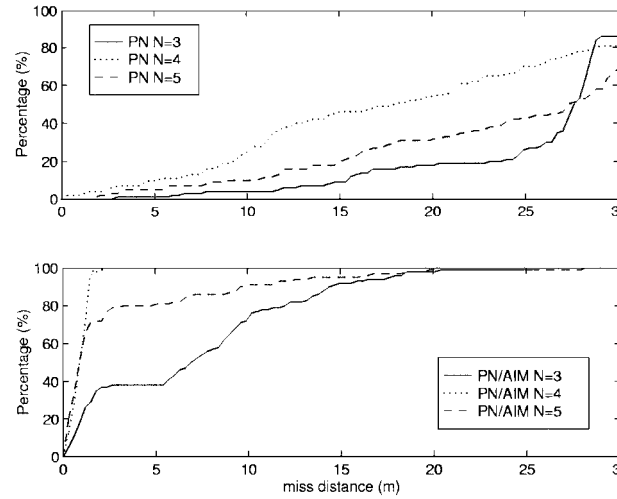

Fig. 11 Miss-distance statistics (case 4).

Similar performances are obtained for the model-CA filter (cases 3 and 4). It is shown in Fig. 10 that the miss-distance characteristics of PN significantly deteriorate for case 3. For case 4 the miss-distance characteristics are shown in Fig. 11. If $N = 3$ is used for the AIM strategy, the target maneuver causes the divergence of range estimation error and significant increases in miss distance. For other choices of guidance gain, the overall intercept performance of PN/AIM is greatly superior to that of PN.

Against maneuvering targets, augmented PN is claimed to perform better than PN. However, this may not be the case if the tracking

filter is not free from the observability problem, as in the case of angles-only measurement. Investigation on this issue is left for further study. The AIM strategy has an ordinary guidance algorithm and a switching mechanism. Conceptually, the switching action is occurred only when the LOS rate is lower than a predetermined value. When the LOS rate is not small (or guidance errors are large), for example, for the maneuvering target case, the AIM strategy may work like the ordinary guidance algorithm because the switch does not turn off. Hence, the AIM strategy can be used for a maneuvering target whenever the basic guidance algorithm can intercept the target.

Conclusions

The proposed adaptive intermittent maneuver strategy is very simple and real-time implementable. Additional variables required to implement these strategies are line-of-sight rate and time to go, but both of them can be easily determined using the filter states. Furthermore, the adaptive intermittent maneuver strategy provides the trajectory modulation necessary for observability enhancement without expending excessive control energy. Although the simulation example in this paper is an atmospheric engagement, the proposed dual-control technique is equally applicable to other homing guidance problems such as guidance of a space interceptor with a passive seeker against a ballistic missile.

Acknowledgments

This work was supported by Agency for Defense Development, Taejon, Republic of Korea, and Automatic Control Research Center at Seoul National University, Seoul, Republic of Korea. The authors are grateful to Hungu Lee and Hyeok Ryu for their technical assistance.

References

[1] Lindgren, A. G., and Gong, K. F., "Position and Velocity Estimation via Bearing Observations," *IEEE Transactions on Aerospace and Electronic Systems,* Vol. AES-14, No. 4, 1978, pp. 564–577.

[2] Aidala, V. J., "Kalman Filter Behavior in Bearings-Only Tracking Applications," *IEEE Transactions on Aerospace and Electronic Systems,* Vol. AES-15, No. 1, 1979, pp. 29–39.

[3] Song, T. L., and Speyer, J. L., "A Stochastic Analysis of a Modified Gain Extended Kalman Filter with Applications to Estimation with Bearings Only Measurements," *IEEE Transactions on Automatic Control,* Vol. AC-30, No. 10, 1985, pp. 940–949.

[4] Song, T. L., Ahn, J. Y., and Park, C., "Suboptimal Filter Design with Pseudo-Measurements for Target Tracking," *IEEE Transactions on Aerospace and Electronic Systems,* Vol. 24, No. 1, 1988, pp. 28–39.

[5] Speyer, J. L., Kim, K. D., and Tahk, M. J., "Passive Homing Missile Guidance Law Based on New Target Maneuver Models," *Journal of Guidance, Control, and Dynamics,* Vol. 13, No. 5, 1990, pp. 803–812.

[6] Tahk, M. J., Ryu, H., and Song, E. J., "Observability Characteristics of Angle-Only Measurement Under Proportional Navigation," *Proceedings of 34th Society of Instrument and Control Engineers Conference*, Vol. 1, Society of Instrument and Control Engineers, Tokyo, Japan, 1995, pp. 1509–1514.

[7] Song, T. L., and Um, T. Y., "Practical Guidance for Homing Missiles with Bearings-Only Measurements," *IEEE Transactions on Aerospace and Electronics Systems*, Vol. AES-32, No. 1, 1996, pp. 434–443.

[8] Casler, R. J., Jr., "Dual Control Guidance Strategy for Homing Interceptors Taking Angle-Only Measurements," *Journal of Guidance and Control*, Vol. 1, No. 1, 1978, pp. 63–70.

[9] Hull, D. G., Speyer, J. L., and Burris, D. B., "Linear Quadratic Guidance Law for Dual Control of Homing Missiles," *Journal of Guidance, Control, and Dynamics,* Vol. 13, No. 1, 1990, pp. 137–144.

[10] Birmiwal, K., and Bar-Shalom, Y., "Dual Control Guidance for Simultaneous Identification and Interception of a Target," *Automatica*, Vol. 20, No. 6, 1984, pp. 737–749.

[11] Speyer, J. L., Hull, D. G., Tseng, C. Y., and Larson, S. W., "Estimation Enhancement by Trajectory Modulation for Homing Missiles," *Journal of Guidance, Control, and Dynamics,* Vol. 7, No. 2, 1984, pp. 167–174.

[12] Hull, D. G., Speyer, J. L., and Tseng, C. Y., "Maximum Information Guidance for Homing Missiles," *Journal of Guidance, Control, and Dynamics,* Vol. 8, No. 4, 1985, pp. 494–497.

[13] Tahk, M. J., and Speyer, J. L., "Use of Intermittent Maneuvers for Miss Distance Reduction in Exoatmospheric Engagements," *Proceedings of 1989 AIAA Guidance and Control Conference,* AIAA, Washington, DC, 1989, pp. 1041–1047.

[14] Tahk, M. J., and Ryu, H., "Adaptive Intermittent Maneuvers of Passive Homing Missiles for Intercept Performance Improvement," *Proceedings of 18th International Council of the Aeronautical Sciences Conference,* Vol. 2, International Council of the Aeronautical Sciences, Beijing, 1992, pp. 1133–1137.

[15] Ryu, H., and Tahk, M. J., "An Improved Switching Scheme of Adaptive Intermittent Maneuver for Passive Homing Missile Guidance," *Proceedings of 35th Society of Instrument and Control Engineers Annual Conference*, Vol. 1, Society of Instrument and Control Engineers, Tokyo, Japan, 1996, pp. 1319–1324.

[16] Nardone, S. C., and Aidala, V. J., "Observability Criteria for Bearings-Only Target Motion Analysis," *IEEE Transactions on Aerospace and Electronic Systems,* Vol. AES-17, No. 2, 1981, pp. 162–166.